CrossMark
click for updates

View Article Online
View Journal

Analyst

Accepted Manuscript

This article can be cited before page numbers have been issued, to do this please use: E. Tenenbaum and E. Segal, *Analyst*, 2015, DOI: 10.1039/C5AN01717C.

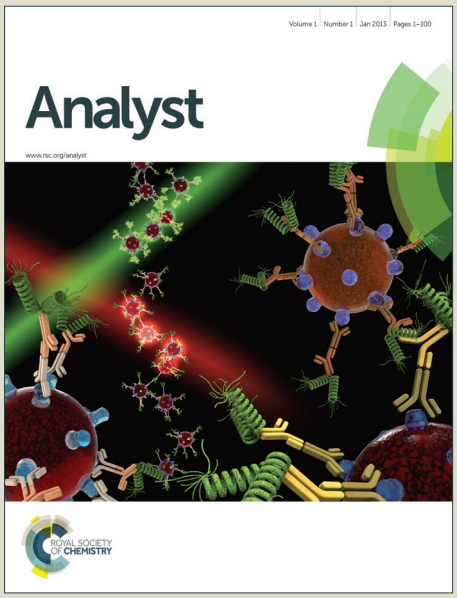

This is an *Accepted Manuscript*, which has been through the Royal Society of Chemistry peer review process and has been accepted for publication.

Accepted Manuscripts are published online shortly after acceptance, before technical editing, formatting and proof reading. Using this free service, authors can make their results available to the community, in citable form, before we publish the edited article. We will replace this *Accepted Manuscript* with the edited and formatted *Advance Article* as soon as it is available.

You can find more information about *Accepted Manuscripts* in the Information for Authors.

Please note that technical editing may introduce minor changes to the text and/or graphics, which may alter content. The journal's standard Terms & Conditions and the Ethical guidelines still apply. In no event shall the Royal Society of Chemistry be held responsible for any errors or omissions in this *Accepted Manuscript* or any consequences arising from the use of any information it contains.

ROYAL SOCIETY OF CHEMISTRY

www.rsc.org/analyst

View Article Online
DOI: 10.1039/C5AN01717C

Published on 23 September 2015. Downloaded by UNIVERSITY OF NEBRASKA on 02/10/2015 09:45:14.

TOC

Sensitive and label-free biosensor for *E. coli* detection, based on a peptidomimetic antimicrobial compound, which is tethered to a nanostructured porous Si optical transducer.

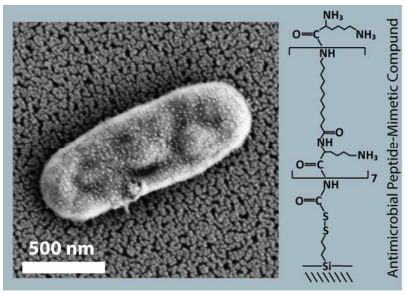

Analyst Accepted Manuscript

View Article Online
DOI: 10.1039/C5AN01717C

Published on 23 September 2015. Downloaded by UNIVERSITY OF NEBRASKA on 02/10/2015 09:45:14.

Optical Biosensors for Bacteria Detection by a Peptidomimetic Antimicrobial Compound

Elena Tenenbaum[a] and Ester Segal[a,b*]

[a]*Department of biotechnology and Food Engineering, Technion – Israel Institute of Technology, Haifa, Israel*

[b]*Russell Berrie Nanotechnology Institute, Technion – Israel Institute of Technology, Haifa, Israel*

*Corresponding author

Received (in XXX, XXX) Xth XXXXXXXXX 20XX, Accepted Xth XXXXXXXXX 20XX

DOI: 10.1039/b000000x

Abstract

In this work we present a label-free optical biosensor for rapid bacteria detection using a novel peptide-mimetic compound, as the recognition element. The biosensor design is based on an oxidized porous silicon ($PSiO_2$) nanostructure used as the optical transducer, functionalized with the sequence K-$[C_{12}K]_7$ (referred as K-7α_{12}), which is a synthetic antimicrobial peptide. This compound is a member of a family of oligomers of acylated lysines (OAKs), mimicking the hydrophobicity and charge of natural antimicrobial peptides. The OAK is tethered to the $PSiO_2$ film and changes in the reflectivity spectrum are monitored upon exposure to *Escherichia coli* (*E. coli*) bacteria suspensions and their lysates. We show that capture of bacterial cell fragments induce predictable changes in the reflectivity spectrum, proportional to *E. coli* concentration, thereby enabling rapid, sensitive and reproducible detection of *E. coli* at concentrations as low as 10^3 cell mL^{-1}. While, for intact bacteria cells, the K-7α_{12}-tethered $PSiO_2$ shows poor capturing ability, resulting in insignificant optical response. The biosensor performance is also studied upon exposure to model Gram positive and negative bacteria lysates, suggesting preferential capture of *E. coli* cell fragments in the presented scheme. These OAK-based biosensors offer significant advantages in comparison to conventional antibody-based assays, in terms of their simple and cost-effective production, while providing numerous possible sequence combinations for designing new

Analyst Accepted Manuscript

View Article Online
DOI: 10.1039/C5AN01717C

Published on 23 September 2015. Downloaded by UNIVERSITY OF NEBRASKA on 02/10/2015 09:45:14.

detection schemes.

Introduction

Rapid detection of infectious microorganisms remains critical in prevention of deadly food- and water-borne disease outbreaks.[1, 2] As current bacteria detection methods rely on lengthy laboratory-based techniques, there is an urgent need for developing biosensing platforms that will allow for rapid detection at a point-of-care.[3, 4]

Antibodies are the gold standard in molecular recognition and are widely incorporated into biosensors and bioassays.[5, 6] However, antibody generation, either through *in vivo* processes or cellular techniques, is expensive and time consuming.[7] Importantly, for analytical applications, antibody-functionalized biosensors may lack the stability needed to detect the target analyte under harsh environments and suffer from undesired conformational changes, which may impede its function.[8] By contrast, antimicrobial peptides (AMPs) are easily synthesized and possess higher intrinsic stability. AMPs are a part of the innate immune system of virtually all organisms, serving as the first line of defence against harmful microorganisms. These peptides are typically amphiphilic and cationic and may have a wide variety of secondary structures.[9-13] Kulagina et al. have previously demonstrated that a multi-AMP array is capable of fluorescence-based cells detection in a concentration-dependant manner with a limit of detection (LoD) $>10^4$ cell mL^{-1}.[10, 14, 15] It has been suggested that the dissimilar binding affinities of different bacteria have the potential to discriminate between different strains of the same species. More recently, Mannoor et al. have developed an impedance-based biosensor, functionalized with the natural AMP magainin, for the detection of infectious agents with an LoD as low as 10^3 cell mL^{-1} with selectivity for pathogenic microorganisms.[16] Uzarski and Mello have demonstrated the ability of AMP array surface to detect and discriminate between five types of lipopolysaccharide (LPS) molecules, originating from the cell walls of different strains of *Escherichia coli* (*E. coli*) and *Pseudomonas aeruginosa*.[12]

In order to deal with protease-digestion sensitivity and production cost issues of naturally occurring AMPs, peptide-mimetic compounds have been designed on the basis of biophysical characteristic of natural AMPs. Synthetic AMP-mimic copolymers, termed OAQs, are a novel group of antimicrobial compounds, composed of oligomers (O) of acylated (A) charged residues (Q).[17] A particular case of OAQs are oligomers of acylated lysines (AK) where Q=lysine (K). The sequence K-$[C_{12}K]_7$ (referred to as K-$7\alpha_{12}$) was shown by Rotem et al. to

Analyst Accepted Manuscript

View Article Online
DOI: 10.1039/C5AN01717C

Published on 23 September 2015. Downloaded by UNIVERSITY OF NEBRASKA on 02/10/2015 09:45:14.

be devoid of antibacterial activity but displayed a high binding capability towards different bacteria, making it a potential candidate for use as a broad-spectrum molecular recognition element.[18]

This study aims to develop a label-free optical biosensor for bacteria detection employing the sequence K-7α_{12} as a novel capture probe. Herein, nanostructured porous silicon (PSi) Fabry-Pérot thin films are used as the optical transducer element, to monitor changes in the reflectivity spectrum upon target binding.[19-26] Our previous work has established the feasibility of antibody-conjugated oxidized PSi ($PSiO_2$) for optical detection of bacteria via 'direct-cell-capture' approach.[5, 6, 27] Exposure of these biosensors to the target bacteria results in their capture onto the $PSiO_2$ surface, inducing predictable changes in the thin-film optical interference spectrum of the nanostructure, i.e., a decrease in the intensity of the reflected light, allowing for rapid detection of low bacterial concentrations. In the present work, the K-7α_{12} sequence is tethered to the $PSiO_2$ scaffold and changes in the reflectivity spectrum are monitored upon exposure to different bacteria and their lysate suspensions. We show that capture of bacterial cell fragments induce changes in the reflectivity spectrum, proportional to *E. coli* concentration, thereby enabling rapid, sensitive and reproducible detection of *E. coli* at concentrations as low as 10^3 cell mL^{-1}.

Experimental

Materials

Highly-doped p-type Si wafers (0.8 mΩ cm resistivity, <100>- oriented, B-doped) were purchased from Siltronix Corp., France. Aqueous HF (48%), ethanol absolute, acetone and hexane were supplied by Merck. Mercaptopropyl-trimethoxysilane (MPTMS), Ethyl-3-(3-dimethylaminopropyl)-carbodiimide (EDC), Morpholinoethanesulfonic acid (MES), MES sodium salt, NaCl, glutaraldehyde and 5,5'-dithiobis(2-nitrobenzoic acid) (DTNB, Ellman's reagent) were obtained from Sigma Aldrich Chemicals, Israel. 2-(2-pyridinyldithio)ethaneamine (PDEA) was obtained from GE Healthcare. Yeast extract, tryptone and Brain heart infusion (BHI) medium were purchased from Becton, Dicknison and Company, USA. *Erwinia carotovora* was generously donated by StePac Ltd., Israel. *Escherichia coli* (*E. coli*, ATCC 8739) and *Listeria innocua* (*L. innocua*, ATCC 33090) were obtained from the American Type Culture Collection (ATTC). Luria-Bertani (LB) medium was prepared by dissolving 5 g of NaCl, 5 g of yeast extract, and 10 g of tryptone in 1 L of deionized

Analyst Accepted Manuscript

View Article Online
DOI: 10.1039/C5AN01717C

Published on 23 September 2015. Downloaded by UNIVERSITY OF NEBRASKA on 02/10/2015 09:45:14.

water. Phosphate buffered saline (PBS) at pH 7.4 was prepared by dissolving 50 mM Na_2HPO_4, 17 mM NaH_2PO_4, and 68 mM NaCl in double-distilled water (ddH_2O, 18 MΩ). Saline solution was prepared by dissolving 0.85 w/v NaCl in ddH_2O.

Preparation of $PSiO_2$

Silicon wafers were electrochemically etched in a 3:1 (v/v) solution of aqueous HF and ethanol for 30 s at a constant current density of 385 mA cm^{-2}. Si with an exposed area of 1.33 cm^2 was contacted on the backside with a strip of aluminum foil and mounted in a Teflon etching cell; a platinum ring was used as the counter electrode. *Caution: hydrofluoric acid is a highly corrosive liquid, and it has to be handled with extreme care and under secured working conditions.* After etching, the surface was rinsed three times with ethanol and once in hexane, and dried under a stream of nitrogen gas. The freshly-etched PSi samples were thermally oxidized in a tube furnace (Thermolyne) at 800ºC for 1 h in ambient air.

Synthesis of K-7α_{12}

The OAK K-7α_{12} and its fluorescently labeled version are a generous gift from Prof. Amram Mor laboratory at the Technion and were produced as described in Marjieh et al.[28] Briefly, the OAKs were prepared by the solid-phase method using 4-methylbenzhydrylamine resin and applying N-(9-fluorenyl)methoxy-carbonyl (Fmoc) active ester chemistry. The OAKs were cleaved from the resin with a mixture of trifluoroacetic acid (TFA):H_2O. The crude compounds were purified to chromatographic homogeneity with a reverse-phase high-performance liquid chromatograph equipped with a mass spectrometer.

Preparation and characterization of OAK-modified $PSiO_2$

The conjugation of the OAKs onto the $PSiO_2$ was carried out by a two-step process. First, $PSiO_2$ samples were incubated with 2% v/v of MPTMS in toluene for 1 h. After the solution was removed, the sample was rigorously rinsed with toluene and acetone and dried under a nitrogen stream. Subsequently, the thiol-modified $PSiO_2$ was incubated with the OAKs solution overnight at 4ºC. The solution was prepared by dissolving 10 µL of OAK (1 mg mL^{-1}), PDEA (22 mM) and EDC (13 mM) in 0.1 M MES buffer (pH=6.0) to a final volume of 60 µL. The resulting solution was allowed to react for 1 h on ice prior to incubation with the thiol-modified $PSiO_2$.

$PSiO_2$ modification was verified using Attenuated total reflectance Fourier transform infrared (ATR-FTIR)

Analyst Accepted Manuscript

View Article Online
DOI: 10.1039/C5AN01717C

Published on 23 September 2015. Downloaded by UNIVERSITY OF NEBRASKA on 02/10/2015 09:45:16.

spectroscopy. Spectra were recorded using a Thermo 6700 FTIR instrument equipped with a Smart iTR diamond ATR device.

The presence of thiol groups on the surface after silanization with MPTMS was verified using Ellman's assay. Ellman's reagent was dissolved in PBS buffer to a final concentration of 0.5 mg mL^{-1}. Subsequently, a volume of 300 µL was allowed to incubate on silanized $PSiO_2$ as well as on neat $PSiO_2$ for 15 min. The resulting solution (200 µL) was collected to a 96-well plate and the absorbance was measured at 412 nm using a plate reader (Thermo Scientific Varioskan).

OAKs conjugation was also studied by Confocal Laser Scanning Microscopy (CLSM) Imaging. Fluorescein-labeled OAKs were immobilized to the $PSiO_2$ as previously described. Images were taken with the Zeiss LSM 700 CLSM, using the Plan-Apochromat 63x/1.40 oil objective. $PSiO_2$ photoluminescence (PL) was excited at 405 nm and observed at 435 nm. The fluorescein-OAK was excited at 488 nm, and its fluorescence was observed at 551 nm. Image acquisition and processing were conducted with the ZEN software (Carl Zeiss).

Preparation of bacteria cultures and their lysates

E. coli and *E. carotovora* bacteria were cultivated in a sterile LB medium (5 mL) overnight at 37ºC (*E. coli*) or 28ºC (*E. carotovora*) under continuous shaking. *L. innocua* was cultivated in a sterile BHI medium (5 mL) overnight at 37ºC under continuous shaking. After overnight growth in the medium, the bacteria concentration was monitored photometrically by reading the optical density (OD) at a wavelength of 600 nm using a spectrophotometer (Ultraspec, Amersham Biosciences). The number of cells is directly proportional to the OD_{600} measurements (1 OD_{600} =10^8 cell mL^{-1}). Afterwards, the suspensions were diluted to the desired concentration in a saline solution. Bacteria lysates were prepared from suspensions by ultrasonication at 4ºC for 15 min, at a constant amplitude of 40% by using Vibra cell VCX 750 instrument (Sonics & Materials Inc., USA). During sonication the sample vessel was immersed in cooling water to avoid temperature increase.

Optical biosensing experiments

All optical experiments were conducted in a custom-made Plexiglas cell while the interferometric reflectance spectra were collected using an Ocean Optics charge-coupled device (CCD) USB 4000 spectrometer (at a wavelength range of 400–1000 nm with a spectral acquisition time of 100 ms) fitted with a microscope

Analyst Accepted Manuscript

View Article Online
DOI: 10.1039/C5AN01717C

Published on 23 September 2015. Downloaded by UNIVERSITY OF NEBRASKA on 02/10/2015 09:45:14.

objective lens coupled to a bifurcated fiber-optic cable. Illumination of the surface and detection of the reflected light were performed along an axis coincident with the surface normal. A tungsten light source was focused onto the center of the sample surface with a spot size of 1 mm^2 and the optical data was collected from this spot throughout the experiment, see Figure S3† for a detailed scheme of the experimental set-up. The obtained reflectivity spectrum is comprised of a series of Fabry-Pérot interference fringes, resulting from reflections at the top and bottom interfaces of the porous thin film. The collected spectra were analyzed by applying fast Fourier transformation (FFT), which results in a single peak with characteristic effective optical thickness (EOT) and intensity. The computed EOT equals *2nL*, where *n* is the effective refractive index and *L* is the physical thickness of the porous layer, and is highly sensitive to the presence of chemical and biological species inside the pores.

OAKs-modified $PSiO_2$ and the proper controls were incubated with *E. coli* suspensions or lysates (10^3 to 10^5 cell mL^{-1}) for 1 h, after which the suspension was removed and the flow cell was flushed with a saline solution for 1 h.

The FFT intensity changes were expressed as the relative intensity ($I\ (t)/I_{baseline}$) or as the intensity decrease, which was calculated using the following equation:

$$\text{Intensity change (\%)} = \frac{\mathrm{I_{baseline}} - \mathrm{I}_t}{\mathrm{I_{baseline}}} \times 100$$

where $I_{baseline}$ is the averaged intensity obtained during baseline establishment at the beginning of the optical experiments and $I\ (t)$ is the measured intensity, and I_t is averaged intensity at the end of the experiment. Similarly, the EOT changes are presented as the relative EOT, $EOT\ (t)/EOT_{baseline}$, where $EOT\ (t)$ refers to the measured EOT at a certain time point and $EOT_{baseline}$ signifies the averaged EOT obtained during baseline establishment.

High-resolution scanning electron microscopy

Top-view images of the biosensors immediately after bacteria detection experiments were taken using a Carl-Zeiss Ultra Plus high-resolution scanning electron microscope (HRSEM), at an accelerating voltage of 1 keV. The biosensors were prepared for observation by fixing the bacteria in a glutaraldehyde solution (2% in 0.1 M PBS) overnight followed by dehydration through an ethanol series (10% to absolute), held at each concentration

Analyst Accepted Manuscript

View Article Online
DOI: 10.1039/C5AN01717C

Published on 23 September 2015. Downloaded by UNIVERSITY OF NEBRASKA on 02/10/2015 09:45:16.

for 30 min. Samples were gold sputtered prior to observation.

Results and discussion

Preparation and characterization of OAK-modified $PSiO_2$ biosensors

Figure 1 presents the synthetic approach for the preparation of the OAK-modified $PSiO_2$ biosensors. First, Si wafers are electrochemically anodized at a constant current density of 385 mA cm^{-2} for 30 s, followed by thermal oxidation. The resulting highly porous films (with a porosity of 78±2%, as determined by gravimetry [5, 29]) are characterized by a typical morphology of interconnecting cylindrical pores with an average diameter of 80±10 nm and a thickness of 7880±60 nm, see Figure S1†, for top-view and cross sectional HRSEM images. In order to immobilize the OAKs to the porous nanostructure, the $PSiO_2$ is first silanized with MPTMS, to introduce thiol groups on the surface (Fig. 1C). ATR-FTIR analysis (Fig. 1F) depicts a peak at 2934 cm^{-1}, assigned to C-H stretching vibrations of the alkanes on the tethered MPTMS molecules. The presence of the thiol groups on the silanized surfaces is determined by using Ellman's reagent (DTNB). The absorbance at 412 nm, assigned to the formation of 5-thio-2-nitrobenzoic acid, is measured for both the silanized surface and the neat $PSiO_2$.[30-32] Indeed, significantly higher absorbance values of 0.7±0.1 are observed for the silanized $PSiO_2$ in comparison to 0.09±0.00 for the neat surface.

Next, the OAK K-7α_{12} is immobilized onto the silanized $PSiO_2$ via its terminal carboxyl group using PDEA and EDC. The attachment of the OAK to the $PSiO_2$ is confirmed by ATR-FTIR. The $PSiO_2$ spectrum after peptide immobilization (Fig. 1F, trace C) depicts several additional peaks, not observed for the neat $PSiO_2$. The peaks at 1634 and 1539 cm^{-1} are assigned to primary and secondary amines, respectively.[33] The peak at 2931 cm^{-1} corresponds to C-H stretching vibrations of the bonds in the lauryl chains.[33, 34]

Analyst Accepted Manuscript

View Article Online
DOI: 10.1039/C5AN01717C

Published on 23 September 2015. Downloaded by UNIVERSITY OF NEBRASKA on 02/10/2015 09:45:14.

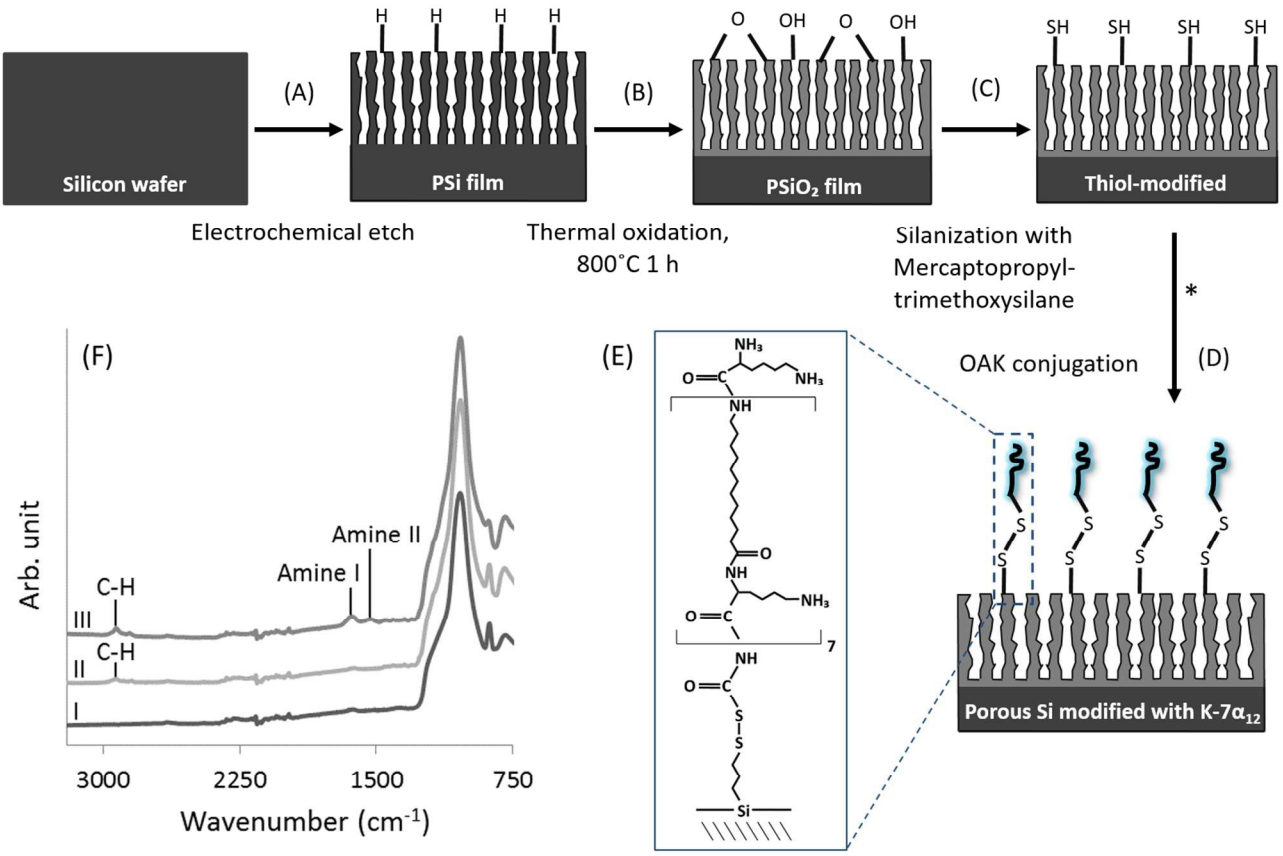

Figure 1: Preparation scheme of OAK-modified $PSiO_2$. (A) PSi Fabry-Pérot nanostructure is prepared by an anodic electrochemical etching; (B) Thermal oxidation at 800°C to produce a $PSiO_2$ scaffold; (C) Silanization with MPTMS to introduce thiol groups onto the surface; (D) Conjugation of the OAK is carried out through its carboxyl terminus to the thiols grafted on the surface; *See Figure S2† for the detailed coupling reaction of the OAK with the MPTMS-modified $PSiO_2$. (E) Schematic representation of the K-7α_{12} OAK-tethered $PSiO_2$. Please note that this scheme is drawn out of scale. (F) ATR-FTIR spectra of (I) neat $PSiO_2$, (II) $PSiO_2$ after silanization with MPTMS, (III) $PSiO_2$ after immobilization of K-7α_{12}.

The peptide K-7α_{12} immobilization is also studied by CLSM imaging using a fluorescein-labeled OAK. Figure 2 depicts z-stack images of $PSiO_2$ after conjugation of fluorescein-OAK and the proper controls. The $PSiO_2$ skeleton photoluminescence (PL) allows to spatially correlate to the fluorescence of the labeled peptides within the porous layer. A strong fluorescence is obtained for the conjugated fluorescein-OAK (see Fig. 2A), confirming successful immobilization of the peptide within the porous nanostructure. When the labeled peptide is incubated with a silanized $PSiO_2$, but the pre-activation of the OAK carboxyl terminus is omitted, no fluorescence is detected (Fig. 2B). Thus, ruling out nonspecific adsorption of the peptide to the silanized

Analyst Accepted Manuscript

View Article Online
DOI: 10.1039/C5AN01717C

surface. Yet, a weak fluorescent signal is observed when a neat oxidized porous film is examined (Fig. 2C), ascribed to non-specific binding of the peptides to the $PSiO_2$ surface. The observed differences in the PL intensity of the $PSiO_2$ may be attributed to the effects of the different surface-attached chemical species[35], as well as to spectral overlap of the fluorescein molecule into the PL detector.

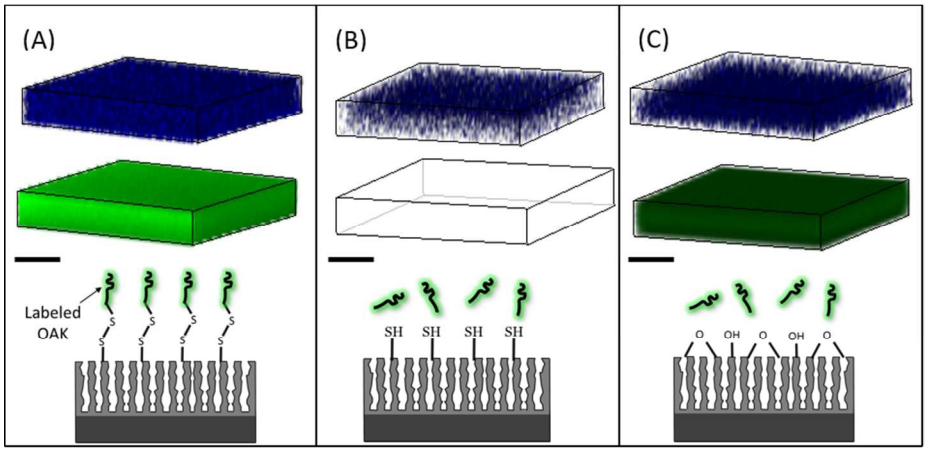

Figure 2: 3D visualization of OAK-modified $PSiO_2$ acquired from stacking of CLSM cross-section images and corresponding schematic illustration. Blue color represents the photoluminescence of the $PSiO_2$ nanostructure and the green color represents the fluorescein-labeled OAK fluorescence. The blue and green signals are presented individually for each sample. (A) Complete bioconjugation; (B) Control experiment, no activation with EDC and PDEA; (C) Control experiment, non-silanized $PSiO_2$. All images were taken under the same acquisition conditions. Scale bar is 5 μm.

Optical detection of bacteria

The OAK-modified $PSiO_2$ are exposed to *E. coli* suspensions while the reflectivity spectra of porous film is monitored in real time and corresponding EOT and intensity values are computed. In all biosensing experiments, the OAK-modified $PSiO_2$ is incubated with saline until a stable baseline of the relative intensity is attained. Next, *E. coli* suspension is introduced and incubated with the biosensor for an hour. The suspension is then removed and the biosensor is washed with saline to minimize possible effect of non-specifically bound species to the OAK-modified surface. A typical biosensing experiment, in which the OAK-modified $PSiO_2$ is exposed to a suspension of *E. coli* bacteria (10^5 cell mL^{-1}), is presented in Figure 3A. The reflected intensity is

Published on 23 September 2015. Downloaded by UNIVERSITY OF NEBRASKA on 02/10/2015 09:45:14.
Analyst Accepted Manuscript

View Article Online
DOI: 10.1039/C5AN01717C

Published on 23 September 2015. Downloaded by UNIVERSITY OF NEBRASKA on 02/10/2015 09:45:16.

slightly reduced upon introduction of the bacteria (see Fig. 3A inset for clarity). However, after the washing step, the signal returns to the initial baseline value, suggesting that the bacteria are removed from the biosensor surface. To validate these results, the sensors are carefully studied by light microscopy immediately after the sensing experiment; no cells are observed on the biosensor surface (data not shown). In our previous studies, in which antibody-based $PSiO_2$ biosensors were employed, we have demonstrated the ability to optically detect intact bacteria cells captured onto the $PSiO_2$ surface with a detection limit of 10^4 cell mL^{-1} (for *E. coli*). [5, 36] We hypothesize that the observed inferior bacteria capturing ability of the tethered OAKs (2.4 kDa), in comparison to tethered antibodies (~150 kDa, Immunoglobulin G [37]), may be attributed to their linear one-dimensional structure and their interfacial arrangement and orientation on the $PSiO_2$ surface.[38] Previous studies have highlighted the complex interplay between AMP tethering conditions and the resulting peptide-bacteria interaction.[38, 39] Thus, the large bacteria cells (1-2 μm [40]) may have limited accessibility to interact properly with the surface-tethered OAKs which is manifested by their instant removal from the surface during the washing step.

In attempt to assert this hypothesis, we have exposed the biosensors to lysed bacteria suspensions (at similar concentrations) in order to facilitate the interaction between the OAKs and the bacteria. As the OAKs' ability to capture bacteria cells is ascribed to their electrostatic interaction with the cell external membrane [28, 41], the numerous small membrane particles formed during bacteria lysis are expected to have improved accessibility and higher surface area to enhance the interaction. Accordingly, bacteria lysis is induced by ultrasonication, which is a commonly employed method for cell disruption, involving the use of ultrasonic waves to generate localized areas of extreme temperature and pressure gradients, that result in acoustic cavitation.[42, 43] Figure 3B depicts the results of a typical biosensing experiment with lysed bacteria suspension (10^5 cell mL^{-1}). Upon introduction of the suspension, a rapid and significant intensity decrease of 14% is observed; followed by an hour incubation with the suspension, during which the signal remains stable. Subsequent washing of the biosensor leads to a minor intensity increase, resulting in a net intensity decrease of 11%. It should be noted that the EOT value remains unchanged during the experiment, indicating that the resulting bacterial lysate contains relatively large particles that are excluded from the porous nanostructure (see Fig. S4†).

Analyst Accepted Manuscript

View Article Online
DOI: 10.1039/C5AN01717C

Published on 23 September 2015. Downloaded by UNIVERSITY OF NEBRASKA on 02/10/2015 09:45:14.

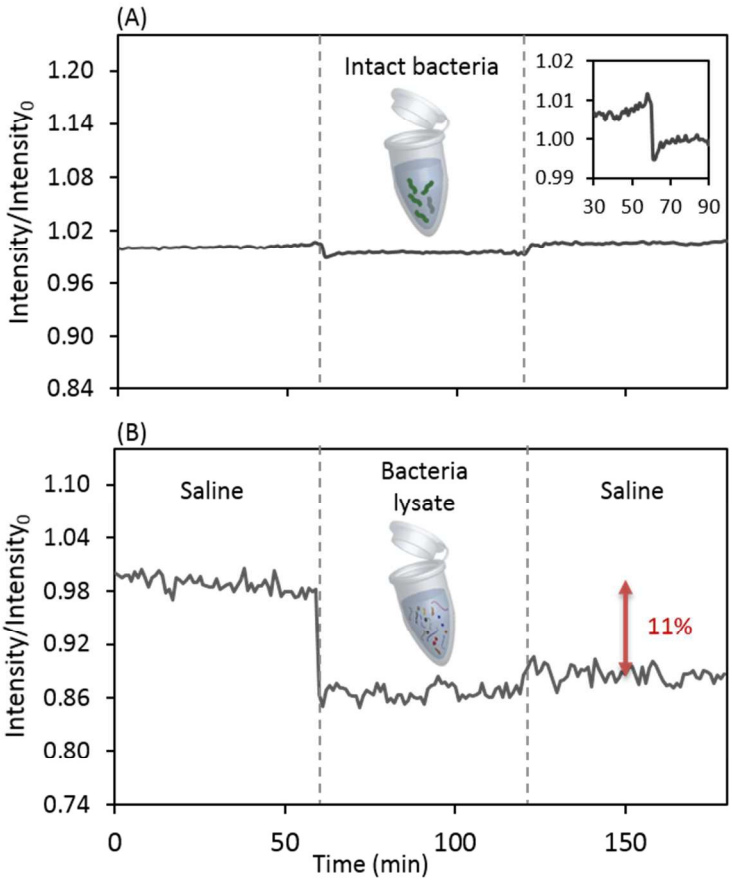

Figure 3: Relative intensity change of the OAK-modified $PSiO_2$ upon exposure of the to *E. coli* bacteria suspensions (10^5 cell mL^{-1}). (A) Intact cells; (B) Lysate.

In order to confirm that this change is induced by the capturing of bacteria lysate onto the OAK-tethered $PSiO_2$ surface, the biosensors are studied by electron microscopy. Figure 4 presents HRSEM micrographs of the biosensor following a sensing experiment. The $PSiO_2$ surface is densely decorated by particles with varying size of ~50-100 nm (see Fig. 4A); careful examination of the nanostructured surface reveals also few captured intact bacteria cells (Fig. 4B). Previous studies by Li et al. have shown similar morphology of captured bacteria wall fragments on top of vancomycin-modified PSi, inducing changes in the optical properties of the PSi microcavity.[26]

Analyst Accepted Manuscript

View Article Online
DOI: 10.1039/C5AN01717C

Published on 23 September 2015. Downloaded by UNIVERSITY OF NEBRASKA on 02/10/2015 09:45:14.

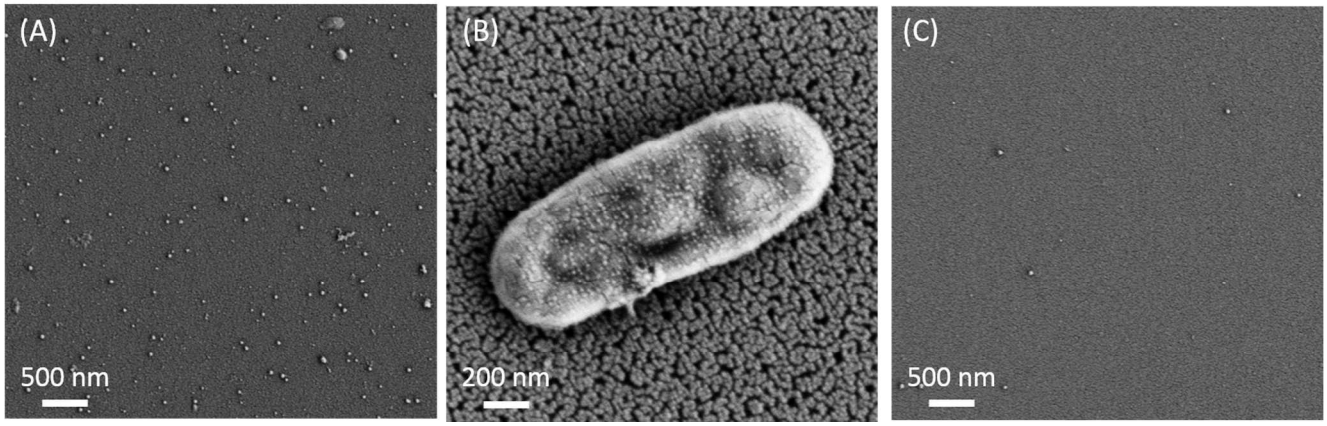

Figure 4: Top-view HRSEM images of (A-B) OAK-modified $PSiO_2$ biosensor after incubation with *E. coli* bacteria lysate suspension (10^5 cell mL^{-1}) followed by a washing step; (C) Non-functionalized $PSiO_2$ (no OAK) after incubation with bacteria lysate.

Control experiments are conducted to eliminate the possibility of non-specific adsorption of bacteria lysate to the surface. In these experiments, neat and thiol-modified $PSiO_2$ (with no OAKs) are exposed to lysate suspension (10^5 cell mL^{-1}). Figure 5A shows that the averaged intensity decrease (of only ~2%) is significantly lower in comparison to the values obtained for the OAK-tethered $PSiO_2$ biosensors (*t*-test, $p<0.005$). This observation is in agreement with HRSEM studies, in which for the $PSiO_2$, examined following exposure to 10^5 cell mL^{-1} and rinsing (Fig. 4C), only few particles are found to be scarcely deposited on the surface. In addition, we also examined the effect of the OAKs immobilization approach on the surface capturing ability. Thus, OAKs are incubated with a thiol-modified $PSiO_2$ (overnight) to allow their adsorption onto the nanostructure. Exposure to bacteria lysate results in minor intensity changes (see Fig. 5A). Therefore, these control experiments demonstrate that properly-tethered OAKs are crucial for the interaction with the lysate particles and resulting profound optical response.

The optical response of the biosensors upon the introduction to different concentrations of *E. coli* lysate suspensions is presented in Figure 5B. The intensity decrease is found to be proportional to the bacteria concentration and linear correlation is demonstrated at a concentration range of 10^3 to 10^5 cell mL^{-1}. At higher bacteria concentrations, the biosensor response deviates from linearity. It should be noted that the measured LoD of this biosensing scheme is 10^3 cell mL^{-1}, one order of magnitude lower than the LoD achieved for

Analyst Accepted Manuscript

View Article Online
DOI: 10.1039/C5AN01717C

monoclonal antibody-based $PSiO_2$ biosensors, which also target *E. coli* and employ a similar experimental setup.[5] Importantly, the LoD we demonstrate here is comparable to the levels previously reported in the literature for AMP-based biosensors, which are in the range of 10^3 to 10^5 cell mL^{-1}.[14, 16, 44-47] However, the majority of these systems require multiple steps of labelling, mostly with fluorescence tags [10, 14, 45, 47, 48]; while the present biosensor offers the significant advantage of a label-free detection.

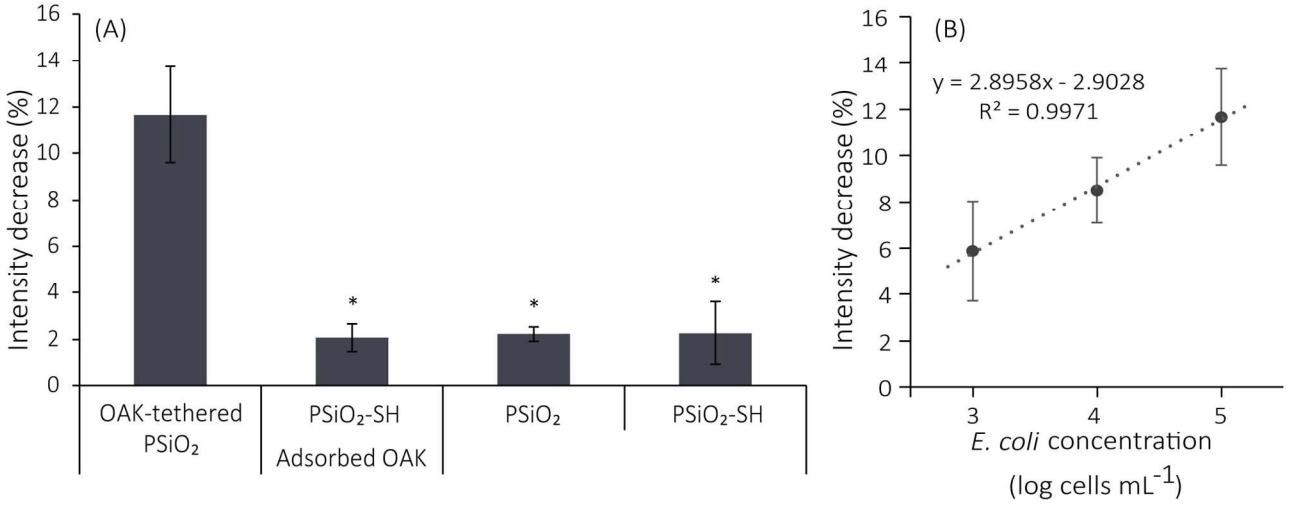

Figure 5: Intensity changes of the sensor upon introduction to *E. coli* lysate suspensions. (A) *E. coli* lysate (at a concentration of 10^5 cell mL^{-1}) on OAK-modified $PSiO_2$ and on control surfaces ($n > 3$ for each experiment). *Significantly different from the OAK-modified $PSiO_2$ (*t*-test, $p < 0.005$); (B) Intensity decrease vs. log (*E. coli* concentration).

The OAK-based biosensor selectivity is studied towards *Listeria innocua* and *Erwinia carotovora,* as Gram positive and Gram-negative model bacteria, respectively. These experiments are performed in a similar manner to the biosensing experiments with *E. coli* lysate. However, for these bacteria species, the biosensor response i.e., intensity decrease, is found to be substantially lower in comparison to results obtained for *E. coli* (see Fig. 6 and Fig. 5, respectively). Moreover, Figure 6 shows that the intensity decrease upon introduction of both *Listeria innocua* and *Erwinia carotovora* lysates onto the biosensor is insignificant when compared to the response of neat $PSiO_2$ nanostructures (with no OAKs). Thus, these biosensing experiments reveal that the K-7α_{12} OAK biosensor exhibits preferential capture of *E. coli* lysate, in comparison to the other studied species. It should be noted that in previous studies when using intact bacteria cells in a capture assay (a spin column filled

Published on 23 September 2015. Downloaded by UNIVERSITY OF NEBRASKA on 02/10/2015 09:45:14.
Analyst Accepted Manuscript

View Article Online
DOI: 10.1039/C5AN01717C

Published on 23 September 2015. Downloaded by UNIVERSITY OF NEBRASKA on 02/10/2015 09:45:14.

with OAKs-linked polystyrene microparticles), the K-7α_{12} did not provide evidence for *E. coli* specificity.[28] These results may be ascribed to significant differences in the assay configuration (bacteria lysate vs. cells, different conjugation chemistry and possible effect of solid support). Thus, further studies are required to elucidate the underlying mechanisms, governing the conjugated OAK-bacteria interactions.

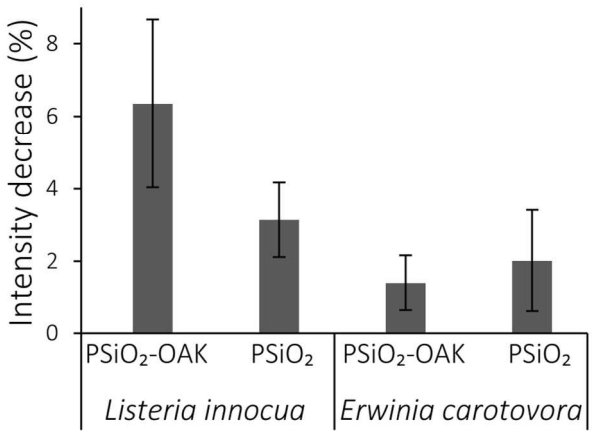

Figure 6: Intensity changes upon introduction of *Listeria innocua* and *Erwinia carotovora* bacteria lysate suspensions (10^5 cell mL^{-1}) onto OAK-modified $PSiO_2$ and neat $PSiO_2$, as a control ($n > 3$ for each experiment).

Conclusions

In this work the OAK sequence, K-7α_{12}, is employed as the capture probe in a $PSiO_2$–based label-free optical biosensor. The OAK is immobilized to the $PSiO_2$ surface via its carboxyl terminus using carbodiimide-coupling chemistry and its successful conjugation is confirmed by ATR-FTIR and confocal microscopy. The OAK-modified $PSiO_2$ biosensors are exposed to *E. coli* bacteria suspensions and their lysates, while their optical response is monitored in real time. This platform exhibits profound and predictable changes in the optical interference spectrum of the $PSiO_2$ with excellent linear correlation to the log of bacteria lysate concentration in the range of 10^3 to 10^5 cell mL^{-1}. Moreover, we achieve a one order of magnitude improvement in the LoD in comparison to our previous studies with monoclonal antibodies.[5] Subsequent, HRSEM studies confirm that the biosensor surface is densely decorated with bacteria lysate particles, which induce the optical response. In contrary, when using intact *E. coli* cells, poor capture onto the $PSiO_2$ surface is attained, possibly due to the limited accessibility of the bacteria cells to the surface-tethered OAKs. The biosensor shows insignificant response to other bacteria species, such as *Listeria innocua* and *Erwinia carotovora*, suggesting that the

Analyst Accepted Manuscript

View Article Online
DOI: 10.1039/C5AN01717C

interaction of *E. coli* cell fragments is preferable in the presented configuration. This OAK-based $PSiO_2$ platform shows potential as an alternative to conventional antibody-based biosensors, offering cost-effective and robust detection schemes.

Acknowledgements

This work was supported by the Israel Science Foundation (Grant 1146/12) and by the NEVET grant administered by the Russell Berrie Nanotechnology Institute (RBNI) and the Lorry I. Lokey Interdisciplinary Center for Life Sciences and Engineering (LS&E). We thank Prof. Amram Mor and Mrs. Fadia Zaknoon (Technion, Israel) for providing the OAKs and for fruitful discussions and comments.

Notes and references

† Electronic Supplementary Information (ESI) available: Supplemental figures/ tables. See DOI: 10.1039/b000000x/

1. P. Leonard, S. Hearty, J. Brennan, L. Dunne, J. Quinn, T. Chakraborty and R. O'Kennedy, *Enzyme Microb. Technol.*, 2003, **32**, 3-13.
2. O. Lazcka, F. J. Del Campo and F. X. Munoz, *Biosens. Bioelectron.*, 2007, **22**, 1205-1217.
3. A. Ahmed, J. V. Rushworth, N. A. Hirst and P. A. Millner, *Clin. Microbiol. Rev.*, 2014, **27**, 631-646.
4. A. Roda, M. Mirasoli, B. Roda, F. Bonvicini, C. Colliva and P. Reschiglian, *Microchim Acta*, 2012, **178**, 7-28.
5. N. Massad-Ivanir, G. Shtenberg, A. Tzur, M. A. Krepker and E. Segal, *Analytical Chemistry*, 2011, **83**, 3282-3289.
6. N. Massad-Ivanir, G. Shtenberg, T. Zeidman and E. Segal, *Advanced Functional Materials*, 2010, **20**, 2269-2277.
7. A. Abbas, L. Tian, J. J. Morrissey, E. D. Kharasch and S. Singamaneni, *Advanced Functional Materials*, 2013, **23**, 1789-1797.
8. D. Saerens, L. Huang, K. Bonroy and S. Muyldermans, *Sensors*, 2008, **8**, 4669-4686.
9. R. E. W. Hancock and H.-G. Sahl, *Nature Biotechnology*, 2006, **24**, 1551-1557.
10. N. V. Kulagina, K. M. Shaffer, G. P. Anderson, F. S. Ligler and C. R. Taitt, *Anal Chim Acta*, 2006, **575**, 9-15.
11. K. Urmann, E. Tenenbaum, J.-G. Walter and E. Segal, in *Electrochemically Engineered Nanoporous Materials*, eds. D. Losic and A. Santos, Springer, Switzerland, 2015, vol. 220, ch. 4, pp. 93-116.
12. J. R. Uzarski and C. M. Mello, *Analytical Chemistry*, 2012, **84**, 7359-7366.
13. M. Zasloff, *Nature*, 2002, **415**, 389-395.
14. N. V. Kulagina, M. E. Lassman, F. S. Ligler and C. R. Taitt, *Analytical Chemistry*, 2005, **77**, 6504-6508.
15. N. V. Kulagina, K. M. Shaffer, F. S. Ligler and C. R. Taitt, *Sensors and Actuators B-Chemical*, 2007, **121**, 150-157.
16. M. S. Mannoor, S. Zhang, A. J. Link and M. C. McAlpine, *Proceedings of the National Academy of Sciences*, 2010, **107**, 19207-19212.
17. I. S. Radzishevsky, S. Rotem, D. Bourdetsky, S. Navon-Venezia, Y. Carmeli and A. Mor, *Nat Biotech*, 2007, **25**, 657-659.
18. S. Rotem, N. Raz, Y. Kashi and A. Mor, *Applied and Environmental Microbiology*, 2010, **76**, 3301-3307.
19. S. Chan, S. R. Horner, P. M. Fauchet and B. L. Miller, *J. Am. Chem. Soc.*, 2001, **123**, 11797-11798.
20. L. De Stefano, L. Rotiroti, I. Rea, L. Moretti, G. Di Francia, E. Massera, A. Lamberti, P. Arcari, C. Sanges and I. Rendina, *Journal of Optics A: Pure and Applied Optics*, 2006, **8**, S540.
21. B. Guan, A. Magenau, S. Ciampi, K. Gaus, P. J. Reece and J. J. Gooding, *Bioconjugate Chemistry*, 2014, **25**, 1282-1289.
22. B. Guan, A. Magenau, K. A. Kilian, S. Ciampi, K. Gaus, P. J. Reece and J. J. Gooding, *Faraday Discussions*, 2011, **149**, 301-317.
23. B. Gupta, Y. Zhu, B. Guan, P. J. Reece and J. J. Gooding, *Analyst*, 2013, **138**, 3593-3615.
24. A. Jane, R. Dronov, A. Hodges and N. H. Voelcker, *Trends in Biotechnology*, 2009, **27**, 230-239.
25. L. L. Jenifer and M. W. Sharon, in *Silicon Photonics for Telecommunications and Biomedicine*, CRC Press, 2011, DOI: doi:10.1201/b11353-7 10.1201/b11353-7, pp. 201-230.
26. L. Sha, H. Jianfeng and C. Lintao, *Nanotechnology*, 2011, **22**, 425502.
27. N. Massad-Ivanir, G. Shtenberg and E. Segal, *Journal of Visualized Experiments*, 2013, DOI: doi:10.3791/50805, e50805.
28. I. Marjieh, O. Meir, F. Zaknoon and A. Mor, *Applied and Environmental Microbiology*, 2015, **81**, 74-80.
29. M. J. Sailor, *Porous Silicon in Practice*, Wiley-VCH, 2012.
30. L. M. Bonanno and L. A. DeLouise, *Advanced Functional Materials*, 2010, **20**, 573-578.
31. H. Peng, W. Chen, Y. Cheng, L. Hakuna, R. Strongin and B. Wang, *Sensors (Basel, Switzerland)*, 2012, **12**, 15907-15946.
32. M. V. Trivedi, J. S. Laurence and T. J. Siahaan, *Current protein & peptide science*, 2009, **10**, 614-625.
33. E. Tenenbaum, N. Ben-Dov and E. Segal, *Langmuir*, 2015, **31**, 5244-5251.
34. T. Böcking, K. A. Kilian, K. Gaus and J. J. Gooding, *Advanced Functional Materials*, 2008, **18**, 3827-3833.
35. M. J. Sailor and E. C. Wu, *Advanced Functional Materials*, 2009, **19**, 3195-3208.
36. N. Massad-Ivanir and E. Segal, in *Porous Silicon for Biomedical Applications*, ed. H. A. Santos, Woodhead Publishing, 2014, DOI: http://dx.doi.org/10.1533/9780857097156.2.286, pp. 286-303.

Published on 23 September 2015. Downloaded by UNIVERSITY OF NEBRASKA on 02/10/2015 09:45:14.

Analyst Accepted Manuscript

View Article Online
DOI: 10.1039/C5AN01717C

37. K. Mitsakakis, A. Tsortos and E. Gizeli, *Analyst*, 2014, **139**, 3918-3925.
38. S. A. Onaizi and S. S. J. Leong, *Biotechnology Advances*, 2011, **29**, 67-74.
39. F. Costa, I. F. Carvalho, R. C. Montelaro, P. Gomes and M. C. L. Martins, *Acta Biomaterialia*, 2011, **7**, 1431-1440.
40. Z. W. El-Hajj and E. B. Newman, *Frontiers in Microbiology*, 2015, **6**, 309.
41. S. Rotem and A. Mor, *Biochimica Et Biophysica Acta-Biomembranes*, 2009, **1788**, 1582-1592.
42. R. B. Brown and J. Audet, *Journal of the Royal Society Interface*, 2008, **5**, S131-S138.
43. P. Piyasena, E. Mohareb and R. C. McKellar, *International Journal of Food Microbiology*, 2003, **87**, 207-216.
44. Z.-M. Dong and G.-C. Zhao, *Talanta*, 2015, **137**, 55-61.
45. H. Etayash, L. Norman, T. Thundat, M. Stiles and K. Kaur, *ACS Applied Materials & Interfaces*, 2014, **6**, 1131-1138.
46. P. B. Lillehoj, C. W. Kaplan, J. He, W. Shi and C.-M. Ho, *Journal of Laboratory Automation*, 2014, **19**, 42-49.
47. J. H. Yoo, D. H. Woo, M.-S. Chang and M.-S. Chun, *Sensors and Actuators B: Chemical*, 2014, **191**, 211-218.
48. S. A. Guralp, I. H. Gubbuk, S. Kucukkolbasi and E. Gulari, *Biochemical Engineering Journal*, DOI: http://dx.doi.org/10.1016/j.bej.2015.04.018.

Published on 23 September 2015. Downloaded by UNIVERSITY OF NEBRASKA on 02/10/2015 09:45:14.

Analyst Accepted Manuscript